

ADSORPTION OF METHYLENE BLUE ONTO ACTIVATED CARBON DEVELOPED FROM BAOBAB FRUIT SHELL BY CHEMICAL ACTIVATION: KINETIC EQUILIBRIUM STUDIES

RADHIA NEDJAI*, MA'AN FAHMI RASHID ALKHATIB,
MD ZAHANGIR ALAM AND NASSERELDEEN AHMED KABBASHI

*Department of Biotechnology Engineering,
Kulliyah of Engineering, International Islamic University Malaysia,
Jalan Gombak, 53100 Kuala Lumpur, Malaysia*

*Corresponding author: radia19@gmail.com.

(Received: 1st November 2020; Accepted: 25th February 2021; Published on-line: 4th July 2021)

ABSTRACT: This article provides results of the usability of baobab fruit shell to produce activated carbons by chemical activation using $ZnCl_2$, H_3PO_4 , and KOH . This study indicated that activated carbon produced from baobab fruit shell fruit can be used as a promising adsorbent for the removal of methylene blue from aqueous solutions. Significant changes on the material surface following the activation process were observed through SEM and FTIR analyses. Scanning electron micrographs of BFS-ACs showed that porous structures were formed during activation, while the FTIR results indicated that the carbons have abundant functional groups on the surface. KOH activation led an activated carbon with a high methylene blue adsorption of 95.54 % and maximum adsorption capacity of 113.63 mg/g, which is directly related to the specific surface area of activated carbons. The adsorption isotherm data were fitted to Langmuir and Freundlich adsorption models. The Langmuir isotherm model showed better fit to the equilibrium data than the Freundlich model. The adsorption process was well described by the pseudo-second-order kinetics. The BFS-ACs is an effective and low-cost adsorbent for the removal of MB from an aqueous solution.

ABSTRAK: Kajian ini memberi input tentang kebolegunaan kulit buah baobab bagi menghasilkan karbon teraktifan melalui aktiviti kimia menggunakan $ZnCl_2$, H_3PO_4 , dan KOH . Karbon aktif daripada kulit buah Baobab ini berpotensi sebagai penyerap bagi menyingkir larutan akueus metilin biru. Perubahan ketara pada permukaan bahan diikuti dengan proses pengaktifan dipantau melalui analisis SEM dan FTIR. Imbasan elektron mikroskop BFS-AC menunjukkan struktur porous terhasil semasa proses pengaktifan. Sementara dapatan FTIR menunjukkan karbon mempunyai banyak kumpulan berfungsi pada permukaan. Pengaktifan KOH menghasilkan karbon aktif menggunakan larutan biru metilin yang tinggi sebanyak 95.54 % dan kapasiti maksimum penyerapan 113.63 mg/g, iaitu berkadar langsung dengan tumpuan kawasan permukaan karbon aktif berkaitan. Data isoterma penyerapan dibina pada model penyerapan Langmuir dan Freundlich. Model isoterma Langmuir lebih padan pada data keseimbangan berbanding model Freundlich. Proses penyerapan menunjukkan lebih kinetik order-kedua-pseudo. BFS-AC sangat efektif dan penyerap murah bagi membuang MB daripada larutan akues.

KEYWORDS: *activated carbon; Baobab fruit shells; methylene blue adsorption; adsorption isotherms; adsorption kinetics*

1. INTRODUCTION

The wide use of dyes in various industries such as textile, paper, rubber, printing, plastic, leather, cosmetics and pharmaceuticals, and food has polluted the environment, especially the aquatic eco-system [1,2]. Dye production dramatically increased in the last years due to the demand in these industries. The presence of dyes in industrial effluents, even at very low concentrations, can cause many significant problems, such as reducing light penetration, which disturbs photosynthesis activity in aquatic life. Moreover, these dyes affect human lives due to the bioaccumulation process which is transferred through the food chain [1,3]. This results from the chemical structure of dye molecules that contain double bonds of olefinic, carbon-nitrogen or nitrogen-nitrogen, and heterocyclic or aromatic rings, which make these dyes hard to break down [4]. Thus, dyes are considered mutagenic, toxic, allergenic, carcinogenic, non-degradable substances [5]. There are more than 700,000 dyestuffs produced per year, which are available with more than 100,000 different chemical structures around the world [3,6]. Methylene blue (MB) is considered the most common azo dyes used for coloring in industry [7]. Because of its harmful effect on water, it is crucial to eliminate it from waste streams before discharge to public water sources.

In order to minimize this dye's impacts on the environment, many technologies have been developed to treat wastewater such as flocculation, coagulation, ozonation, chlorination, anodic oxidation, and electrooxidation. However, these techniques are costly and frequently become secondary sources of pollution [8]. Many studies revealed that adsorption by solid adsorbents presents the advantages of high efficiency, simple design, and low initial costs [7]. The activated carbon is one of the most effective adsorbents for the removal of water pollutants. Using agricultural by-products for the production of activated carbon provides an environmentally credible alternative to coal, pitch, petroleum, and coke. It minimizes the production cost of activated carbon since it is inexpensive and abundant. Moreover, it is an efficient solution to the discarding of huge amounts of waste.

Various agricultural by-products have been used as a precursor in producing activated carbon for the removal of methylene blue from the wastewater such as pine cone [1], bamboo [9], karanj (*Pongamia pinnata*) fruit hulls [10], prawn shells [11], cashew nut shells [7], tea fruit peel residues [12], tea (*Camellia sinensis L.*) seed shells [13], dabai (*Canarium odontophyllum*) nutshells [14], date pits [15], cola nutshells [16], bitter kola (*Garcinia kola*) nutshells [17], baobab fruit shells (*Adansonia digitata L.*) [18], palm kernel shell [19], lapsi seed stone [20].

Adsorption capacity is one of the most important characteristics of activated carbon. It is affected by the inherent nature of the precursor and the activation process which is determined by different conditions such as the activating agents, temperature, and activating time [20]. Activating agents have a great influence on the surface and pore formation of produced activated carbon. Various chemical agents proposed for chemical activation such as potassium hydroxide [17,21,22], zinc chloride [17,19], phosphoric acid [17,22,23], potassium carbonate [24,25], calcium chloride [20], and sodium hydroxide [26,27]. Each of these reagents creates different influences on pore development and has its distinctive safety concerns that influence the application of the produced activated carbon. For example, the H_3PO_4 and $ZnCl_2$ have boiling points of 213 °C and 732 °C, respectively, could decompose at the activation temperature and cause toxic fumes. The KOH, on the other hand, has a boiling point of 1327 °C, which is higher than the typical activation temperatures [28].

Baobab fruit shell is not only an organic waste component that has no economic benefits but is also creates problems with waste treatment and disposal. Baobab fruit shells are an abundant new precursor for the production of activated carbon as they contain high volatile

matter (86.73 %) and low ash (5.57 %) [29]. Therefore, the main focus of this study is to utilize Baobab Fruit Shell (BFS) as a renewable and low-cost precursor for producing a high surface area activated carbon (BFS-ACs) by chemical activation using H_3PO_4 , KOH, and $ZnCl_2$. Activated carbon could appropriately be prepared from the BFS which would lead to its valuable application. To the best of our knowledge, there has been no study reported on the influence of activating agents on the adsorption capacity of activated carbons made from BFS. Hence, the main objective of this research was to produce high surface area microporous activated carbon from baobab fruit shells using different chemical activation reagents and to study their effects on the adsorption of methylene blue (MB). The adsorption properties of the prepared BFS-ACs was studied with Methylene Blue in aqueous solution under equilibrium and kinetic conditions to obtain the associated adsorption parameters.

2. MATERIALS AND METHODS

2.1 Materials

BFS were used as a precursor for the preparation of activated carbon and were acquired from West Sudan. The samples BFS were washed several times with tap water and finally with distilled water to remove any impurities. The shells were dried in the oven at 105 °C for dehydration until a constant weight was obtained. Then, they were ground and screened to obtain particles of the size of 1 mm.

Phosphoric acid (H_3PO_4), potassium hydroxide (KOH), and zinc chloride ($ZnCl_2$) were utilized as chemicals reagents for the activation process, which were acquired from Macron Fine Chemicals (USA), Sigma-Aldrich (Malaysia), and R&M Chemicals (Malaysia), respectively. Nitrogen gas (99.95 %) was purchased from Fuelink Marketing Sdn. Bhd. (Selangor, Malaysia), that was used for the inert atmosphere during carbonization. Iodine was acquired from Univar (UK). Potassium iodide was purchased from Ducheda Biochemie (Malaysia). All other chemicals of analytical grade were utilized throughout the experiments.

2.2 Preparation of Adsorbate

Methylene blue (C.I.52015) StainPur was obtained from System. Methylene blue solution (1000 mg/L) was prepared through dissolving 1.127 g methylene blue with distilled water in the volumetric flask of 1 L [30]. The prepared solution was diluted with distilled water to obtain the required concentrations for each experiment.

2.2 Activated Carbon Preparation

For the activation process, 10 g of dried BFS was mixed with different chemical reagents ($ZnCl_2$, KOH, or H_3PO_4) at an impregnation ratio of 1:1. Then, 80 mL of distilled water was added and agitated utilizing a rotary shaker for 1 hour at 50 °C. The samples were then oven-dried at 100 °C for 16 hours to get a thick paste. Later, the samples were inserted into a Carbolite horizontal tube furnace at 10 °C/min at 500 °C for 60 min under continuous flowing nitrogen gas (99.95 %). The carbonization step was conducted in a Lenton horizontal tubular quartz reactor (England, UK) consisting of a Carbolite horizontal tube electrical furnace (Model CTF, UK) with a maximum operating temperature of 1200 °C, a pressure regulating valve, and a controller (Fig. 1). The resulting products were finally moved to the desiccator to cool down. The weight of produced activated carbons (BFS-ACs) was measured [31].

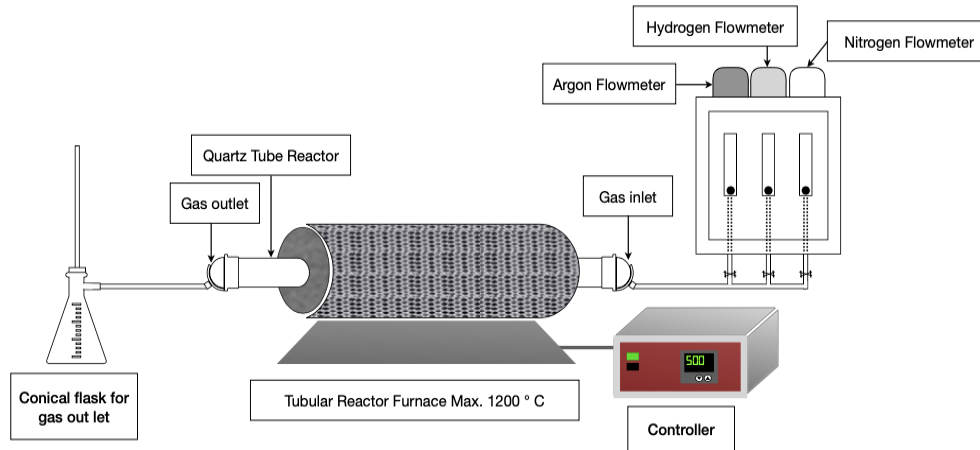


Fig. 1: Schematic diagram of the experimental setup for BFS-ACs production.

2.4 Activated Carbon Purification

BFS-ACs were washed utilizing 50 mL of 0.5 M HCl to remove any residual of the dehydrating agents and any ash in the samples. The BFS-ACs were frequently washed with warm distilled water until a constant pH was achieved and were dried at 110 °C for 24 hours using a vacuum oven [31].

2.5 Characterization of the Carbonized Carbon

The following characteristics of the carbonized BFS carbon were determined:

2.5.1 Proximate Analysis

The ash content was determined by ASTM D 2866-83 [32], and the moisture content of BFS-ACs was measured based on a procedure by ASTM D 2867-91 [33].

2.5.2 Determination of the Yield

Activated carbon yields were calculated based on the equation:

$$\text{Yield}(\%) = \frac{W_f}{W_i} \times 100 \quad (1)$$

where W_f is the dry mass of final activated carbon in grams, which is taken after the activated carbon is produced. While W_i is the dry mass of BFS in grams, which is taken at the beginning of the experiment [34].

2.5.3 Determination of the Bulk Density

The density of the prepared product was determined by wrapping five grams of activated carbon in a plastic bag. Then, the sample was placed in a 500 mL graduated cylinder that contained water. The difference in the level of water was measured. The density was calculated using the equation [35]:

$$\text{Bulk density}(g/cm^3) = \frac{\text{Activated Carbon weight}(g)}{\text{Volume}(cm^3)} \quad (2)$$

2.5.4 Determination of Iodine Number

Iodine number was carried out following the procedure by Vunain et al. [36]. Potassium iodide (4.10 g) was precisely weighed and mixed with 2.70 g of iodine crystals to prepare one liter of iodine solution. Standardization of the stock solution was done using a standard

solution of sodium thiosulfate ($\text{Na}_2\text{S}_2\text{O}_3$). Five hundred milligrams of the produced activated carbon were transferred to Erlenmeyer flasks of 250 mL and was mixed with 100 mL of iodine solution. The mixture was left stirring using a rotary shaker at a rapid speed, and then the mixture was filtered using filter paper. Only 20 mL of the filtrate was transferred into a clean Erlenmeyer flask, where it was titrated with standardized 0.1 N sodium thiosulfate ($\text{Na}_2\text{S}_2\text{O}_3$) until the yellow color disappeared. An amount of starch solution (around 1 mL) was added, and the titration continued pending the disappearance of the blue indicator color. The amount of iodine adsorbed per milligram, I (mg/g) was plotted against the concentration of iodine in the filtrate (C). The residual iodine concentration (C) was calculated and the whole procedure of the experiment was repeated using a different mass of activated carbon if the value of (C) was not within the range of 0.008-0.04 mol/L. The I and C values were calculated by equations (2) and (3), respectively [37].

$$I \left(\frac{\text{mg}}{\text{g}} \right) = (N_1 \times 126.93 \times V_1) - \left(\left(\frac{V_1 + V_{\text{HCl}}}{V_f} \right) \times (N_2 \times 126.93 \times V_2) \right) / W_C \quad (3)$$

$$C = N_2 \times V_2 \quad (4)$$

where N_1 is the normality of the iodine solution, N_2 is the normality of sodium thiosulfate solution, V_1 is the additional volume of iodine solution, V_2 is the volume of sodium thiosulfate solution consumed, V_{HCl} is the additional volume of 5 % HCl , V_f is the filtrate volume used in titration and W_C is the activated carbon weight.

2.5.5 Fourier Transform Infrared (FTIR)

Fourier transform infrared (FTIR) spectroscopic was utilized to analyze the surface chemistry of prepared activated carbons (BFS-ACs) and the raw material (BFS) applying a Perkin Elmer Frontier model FTIR-spectrometer. Before starting the analysis, the dry samples were combined with KBr powder. Then, the mixtures were compressed into capsules that were utilized for analysis. The % of absorbance of samples was recorded over 400 to 4000 cm^{-1} .

2.5.6 Screening Electron Microscopy (SEM)

The morphological structure of the BFS and prepared BFS-ACs was observed utilizing scanning electron microscopy (SEM). The samples were prepared on a carbon tape and images were taken using JEOL-IT100 SEM instrument (JEOL, Japan). Pore size measurements were carried out using the measurement tool equipped with the JEOL IT100 SEM (InTouchScope™ version 1.060).

2.6 Batch Equilibrium Studies

In experiments of batch equilibrium adsorption, 0.3 g of different BFS-AC samples were weighed and taken in several conical flasks. Methylene blue solution (100 mL) at different concentrations (25, 50, 100, 200, 300, 400 mg/L) was added. Then, the flasks were placed in a rotary shaker for various contact times (i.e. 5, 10, 15, 30, 60, 120, 180 min) at 120 rpm at room temperature ($27 \pm 1^\circ\text{C}$). The solution was filtered and the residual concentration of methylene blue was determined at 660 nm using a UV/vis spectrophotometer.

The amount of methylene blue adsorbed by biosorbent was calculated using the following equation:

$$q_e = \frac{(C_i - C_f)V}{w} \quad (5)$$

where the amount of methylene blue adsorbed per gram of biosorbent at equilibrium (mg/g) is represented by (q_e), the initial methylene blue concentration is represented by C_i (mg/L), the final or equilibrium methylene blue concentration is represented by C_f (mg/L), the volume of methylene blue solution in the flasks is represented by V (L) and the weight of biosorbent used is represented by W (g) [38].

The difference between methylene blue concentration before and after adsorption ($C_i - C_f$) to the initial concentration of methylene blue in the aqueous solution (C_i) is known as the percentage of methylene blue uptake, and it may be estimated using the following equation:

$$Removal (\%) = \frac{(C_i - C_f)}{C_i} \times 100 \quad (6)$$

3. RESULTS AND DISCUSSION

3.1 Characterization of Adsorbent (BFS-ACs)

3.1.1 Effects of Activating Agents on the Yield of AC

The yield of prepared BFS-ACs was determined, and the results are shown in Table 1. Rendering to the results, the yield of BFS-ACs ranged from 30.3 % to 34.6 %, obtained under the same conditions (500 °C for 1 h). All the data presented are the average of three replicates. The highest yield was obtained by phosphoric acid (H_3PO_4) with 30.3 %, followed by zinc chloride ($ZnCl_2$) with 33.6 %, and potassium hydroxide (KOH), respectively. At a higher temperature, more volatiles and polymeric structures decompose such as cellulose, lignin, and hemicellulose are liberated causing a lower yield.

The existence of H_3PO_4 over the activation process favors the transformation of aliphatic to aromatic compounds, dehydration, promotes depolymerization, and redistribution of constituent biopolymers, consequently, raising the yield of activated carbon [34].

Table 1: Yield, moisture content, ash content, bulk density and iodine number of prepared BFS-ACs

| Adsorbent | Yield (%) | Ash content (%) | Moisture content (%) | Bulk density (g/cm ³) | Iodine Number (mg/g) |
|--------------------------------|-----------|-----------------|----------------------|-----------------------------------|----------------------|
| ZnCl ₂ | 33.663 | 17.3 | 1.15 | 0.3 | 1213.45 |
| H ₃ PO ₄ | 34.396 | 17.7 | 5.17 | 0.3 | 1248.35 |
| KOH | 30.377 | 14.3 | 1.63 | 0.3 | 1227.41 |

3.1.2 Ash and Moisture Content

Ash content and moisture content were determined due to their importance, and the results are also reported in Table 1. Ash content consists of inorganic substances that lead to a rise in hydrophilic nature and could cause catalytic effects leading in restructuring pending regeneration of AC [39]. Overall, ash content ranges from 1 to 20 %, which depends on the type of raw material, and the activating agents used in the activation process. High ash content affects adsorptive capacity and reduces the mechanical strength of carbon, therefore, it is unsuitable for the AC [40]. The highest value of ash content was that AC produced using H_3PO_4 , whereas the lowest value of ash content was that AC produced using KOH.

The amount of water physically associated with activated carbon was determined by calculating the moisture content, which depends on various porous characteristics like the pore volume and surface area. Generally, when activated carbon is exposed to air, that with high surface areas absorb more moisture. Some studies reported that the rate of absorption of contaminant moisture increases with lower moisture content. The values of 1.15 %, 5.17 %, and 1.63 % were obtained for $ZnCl_2$, H_3PO_4 , and KOH, respectively.

The bulk density is the mass of the activated carbon particles divided by the volume they occupy. It is an important characteristic of activated carbon for a densified bed or gas storage application. The bulk density of the prepared BFS-ACs is 0.3 g/cm^3 .

3.1.3 Iodine Number

Iodine number, also called iodine adsorption, is considered one of the best methods to determine the capacity of adsorption and the quality of activated carbon. It is frequently utilized because of its simplicity and rapidity [36]. The higher iodine number signifies a great probability that activated carbon has a very large micropore structure and has a high surface area for the adsorption to take place [37]. Table 1 displays the variation of the iodine number for BFS-ACs prepared with different activating agents. H_3PO_4 impregnated activated carbon had the highest iodine number (1248 mg/g), while the lowest iodine number was obtained from activated carbon impregnated with $ZnCl_2$ (1213 mg/g). Therefore, the iodine number of carbons prepared by activation processes were in the order of $H_3PO_4\text{-AC} > \text{KOH-AC} > ZnCl_2\text{-AC}$.

3.1.4 Morphological Structures of the Activated Carbon

After activation in the tube furnace with the three different activating agents ($ZnCl_2$, KOH, and H_3PO_4), the samples were observed utilizing a scanning electron microscope (SEM) and the results are presented in Fig. 2.

The morphological structure of the raw BFS and prepared activated carbons were observed using the SEM technique. SEM reveals the raw material (Fig. 2a) have the lowest original pores structures. However, the treated-BFS with different activating agents ($ZnCl_2$, KOH, and H_3PO_4) contains more porous structures that are honeycomb-shaped with different pore sizes owing to the degradation of the cellulosic fraction, which is affected by the pyrolytic decomposition of biomass by influences of activating agents.

There is no difference in the material that has been used as raw material to prepare the AC, however, there are morphological differences between the prepared AC obtained which refer to tremendous differences in the activating agents that were used and their different reaction mechanisms. $ZnCl_2$ encouraged the elimination of water molecules from the lignocellulosic structures of the raw materials, while H_3PO_4 combined chemically into the lignocellulosic structures. Therefore, there is no selective elimination of carbon over the activation which ameliorates the yields. The KOH mechanism is more complex and contains the disintegration (almost explosively) of the structure following intercalation and some gasification by oxygen molecules of hydroxide as well [41].

Many mesopores with an irregular yet extremely porous structure were occupied by the KOH-AC structure (Fig. 2b). On the other hand, H_3PO_4 and $ZnCl_2$ activated carbons (Fig. 2c and 2d) clearly show developed honeycomb as strongly defined pores with regularity and cavities compared to raw BFS and $ZnCl_2\text{-AC}$. Zinc chloride activated carbon exhibited a high macropore size with an average of $44.21 \mu\text{m}$, followed by KOH with an average of $42.24 \mu\text{m}$, and H_3PO_4 with an average of $27.90 \mu\text{m}$. Besides, the pores in the KOH micrograph are greater than in the H_3PO_4 and $ZnCl_2$ micrographs. Therefore, there is great potential to absorb and trap methylene blue.

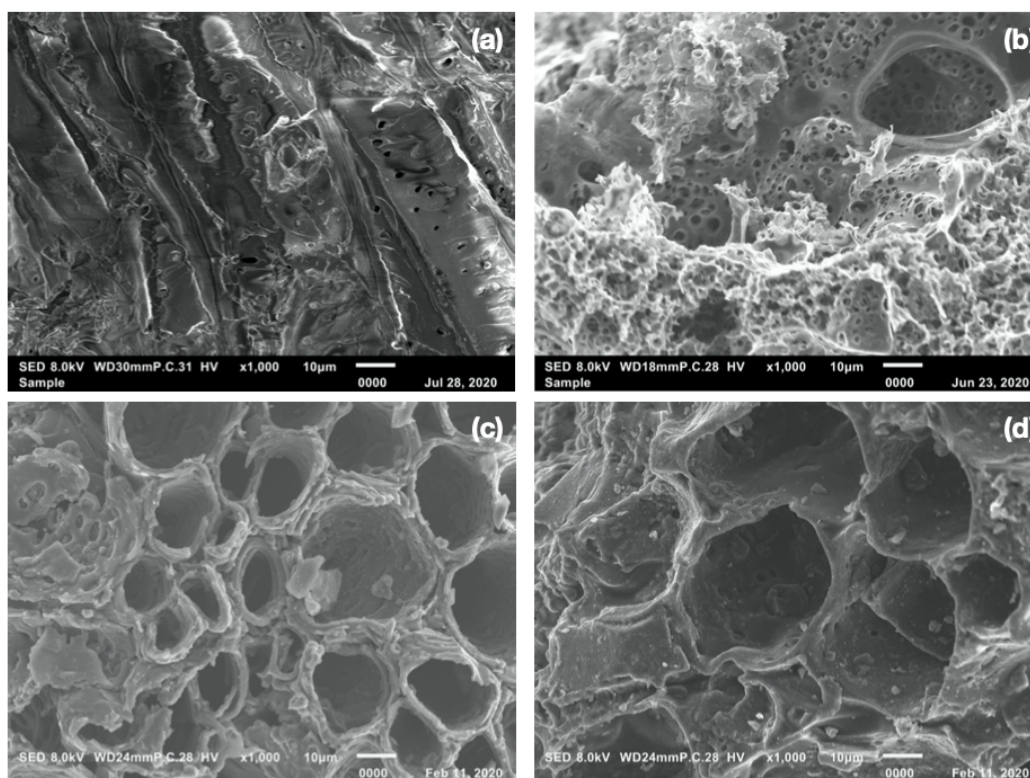


Fig. 2: SEM photomicrographs of (a) BFS; (b) AC produced from BFS using KOH; (c) AC produced from BFS using H_3PO_4 ; (d) AC produced from BFS using ZnCl_2 (magnification scale $\times 1000$).

3.1.5 Surface Chemistry

The IR spectrum of raw BFS and BFS-ACs samples were recorded using a KBr disk in conjunction with a Perkin-Elmer infrared spectrophotometer. Figure 3 displays the results, and the graphs were taken between the wavenumbers of 4000 cm^{-1} and 400 cm^{-1} . As can be seen, the raw BFS spectrum exhibited more absorption peaks than the BFS-ACs spectrum, where several peaks that were present in the raw BFS disappeared once the activation step was performed, owing to the elimination of heat-sensitive functional groups at high temperatures and volatiles.

For the raw BFS, the broad band at 3285.18 cm^{-1} is characteristic of a stretching vibration of hydrogen-bonded (O-H) hydroxyl groups of cellulose, pectin, and lignin [18]. The peak appearing at 2889.65 cm^{-1} is described to (C-H) symmetric stretching and ($-\text{CH}_2$) alkyl groups. The small bands observed at 2160 cm^{-1} and 2031 cm^{-1} are due to the presence of ($\text{C}\equiv\text{N}$) stretching [18,34,36]. The band at around 1613.83 cm^{-1} is the ($\text{C}=\text{O}$) stretching vibration due to bonds of esters and phenols [42], which disappeared in BFS-ACs. A comparatively low-intensity peak at 1367 cm^{-1} is owing to the presence of ($\text{C}-\text{O}-\text{C}$) stretching or $\text{C}=\text{C}$ stretching that can be ascribed to the existence of ester, ether, and phenol. A peak situated at around 1033.37 cm^{-1} is the characteristics of anhydrides ($\text{C}-\text{O}$), which is observed also in ZnCl_2 -AC and disappeared completely in KOH and H_3PO_4 . The principal functional groups in BFS are hydroxyl groups, carbonyl groups and carboxyl groups.

FTIR spectrum of all prepared BFS-ACs shows broad weak peaks around $3900\text{--}3600\text{ cm}^{-1}$. For H_3PO_4 and KOH activated carbons present a similar FTIR spectrum, which indicates the identical type of surface functional groups. The FTIR spectrum of BFS-ACs shows distinguished characteristic peaks as follows: 3333.13 cm^{-1} (vibrations of O-H

groups), 2886.24 cm^{-1} (stretching of C–H), 2161.38 cm^{-1} (stretching of C≡C), 1574.71 cm^{-1} (stretching of C=C), 1255.45 cm^{-1} (stretching of C–O), respectively. KOH activated carbon presents peaks with slighter intensity as contrasted to H_3PO_4 , which demonstrates a lower quantity of functional groups in KOH. As stated by Puziy et al., the band obtained by H_3PO_4 at 1179 cm^{-1} can be assigned to the phosphorous-containing group P–O, O–C stretching vibrations in P–O–C linkage, and P=OOH [43]. On the other hand, the ZnCl_2 activated carbon, the very small bands around 2358 and 1087 cm^{-1} are related to the C≡N and the C–O stretching, respectively.

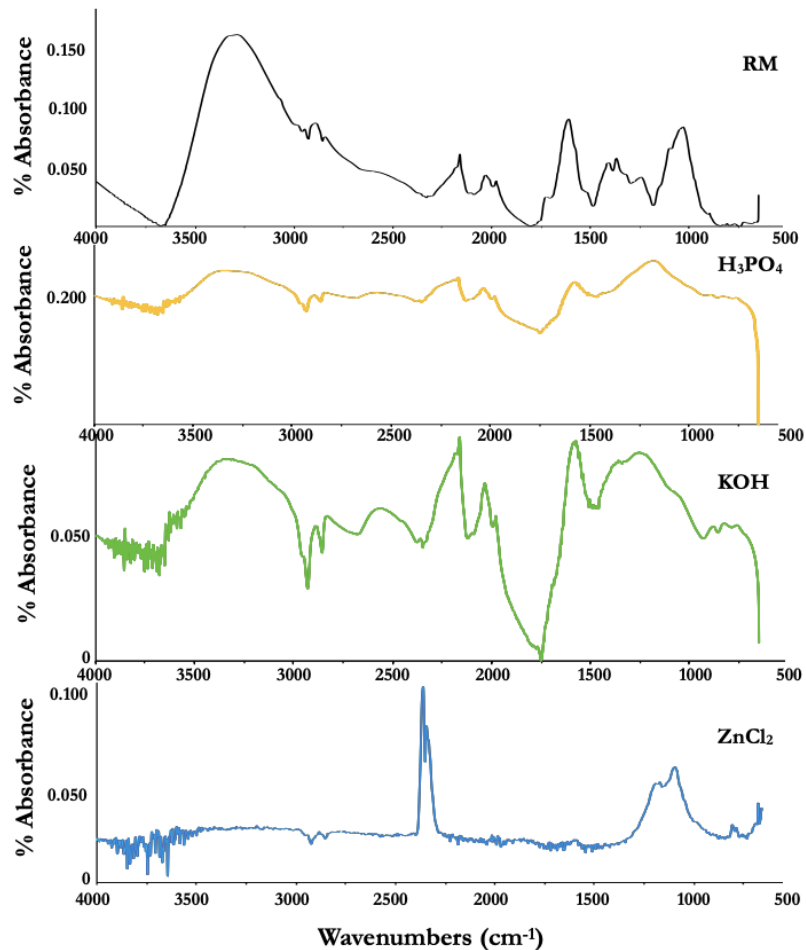


Fig. 3: Fourier transform infrared spectrum for raw Baobab fruit shells and BFS-derived activated carbons (BFS-ACs).

3.2 Adsorption Process

3.2.1 Effect of Initial Methylene Blue Concentration

For the adsorption process, the prepared BFS-ACs were employed as adsorbents to study the effect of chemical activating agents on the adsorption of methylene blue. The adsorption studies were performed using adsorbent of 3 g/L at agitation speed of 120 rpm at $27\pm 1\text{ }^\circ\text{C}$. Figure 4 shows the effect of initial concentration on methylene blue adsorption, which were carried out at different initial dye concentrations (25 to 400 ppm). The results revealed that the actual amount of MB adsorbed (mg/g) increased with the increase in the initial dye concentration. The analysis of these results shows that the methylene blue uptake efficiencies of the prepared activated carbons were almost similar at low concentrations and significantly different at high concentrations.

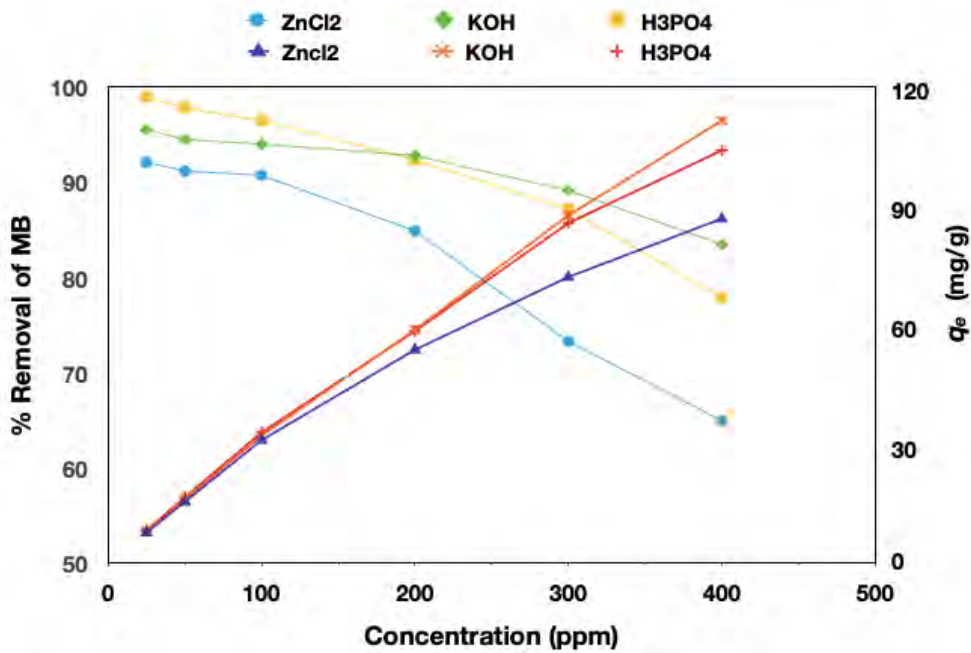


Fig. 4: Effect of initial concentration on methylene blue adsorption (adsorbent dose = 3 g/L, stirring speed = 120 rpm, temperature = 27 ± 1 °C, volume of solution = 100 mL).

From the graph, it can be seen that the percentage of methylene blue removal decreased with the increase of the initial dye concentration. Where a high concentration of methylene blue contributes to higher interaction between methylene blue and adsorbent. Similar results were reported in the literature for the removal of methylene blue [44].

Generally, a high efficiency of removal of methylene blue was observed in KOH activated carbon, followed by H₃PO₄ and ZnCl₂ as have been revealed by another study [17]. However, at low concentration (25, 50, and 100 ppm), the efficiency of the removal of methylene blue by H₃PO₄ activated carbon reached to 98.97 %, 97.84 %, and 96.48 %, respectively, which is higher than the efficiency of the two other prepared activated carbons. Whereas, at high concentration (200, 300, and 400 ppm), the efficiency of dye removal by KOH activated carbon attained was 92.82 %, 89.1 %, and 83.48 %, respectively, which is higher than the efficiency of H₃PO₄ and ZnCl₂ activated carbons. Significant uptake of KOH compared to ZnCl₂ and H₃PO₄ could be explained by differences in the morphological structure of the activated carbon, as shown in Fig. 2.

3.2.2 Effect of Contact Time on Methylene Blue Adsorption

The adsorption data for the removal of methylene blue dye versus contact time at different initial concentrations is demonstrated in Fig. 5. The adsorption studies of MB into BFS-ACs were followed over 3 hours. In general, most of the methylene blue removal takes place during the first 30 minutes. The equilibrium adsorption was achieved after 1 hour and no remarkable changes being observed for longer contact time. The results show that the adsorption capacity of methylene blue on BFS-ACs dramatically augmented during the preliminary period and thereafter with slower speed. The adsorption capacity is highly prompted by the number of available active sites, which are numerous at first; consequently, the adsorbate extends the active sites easily. Afterward, the number of active sites reduces, and the adsorbent surface turns out to be saturated [45].

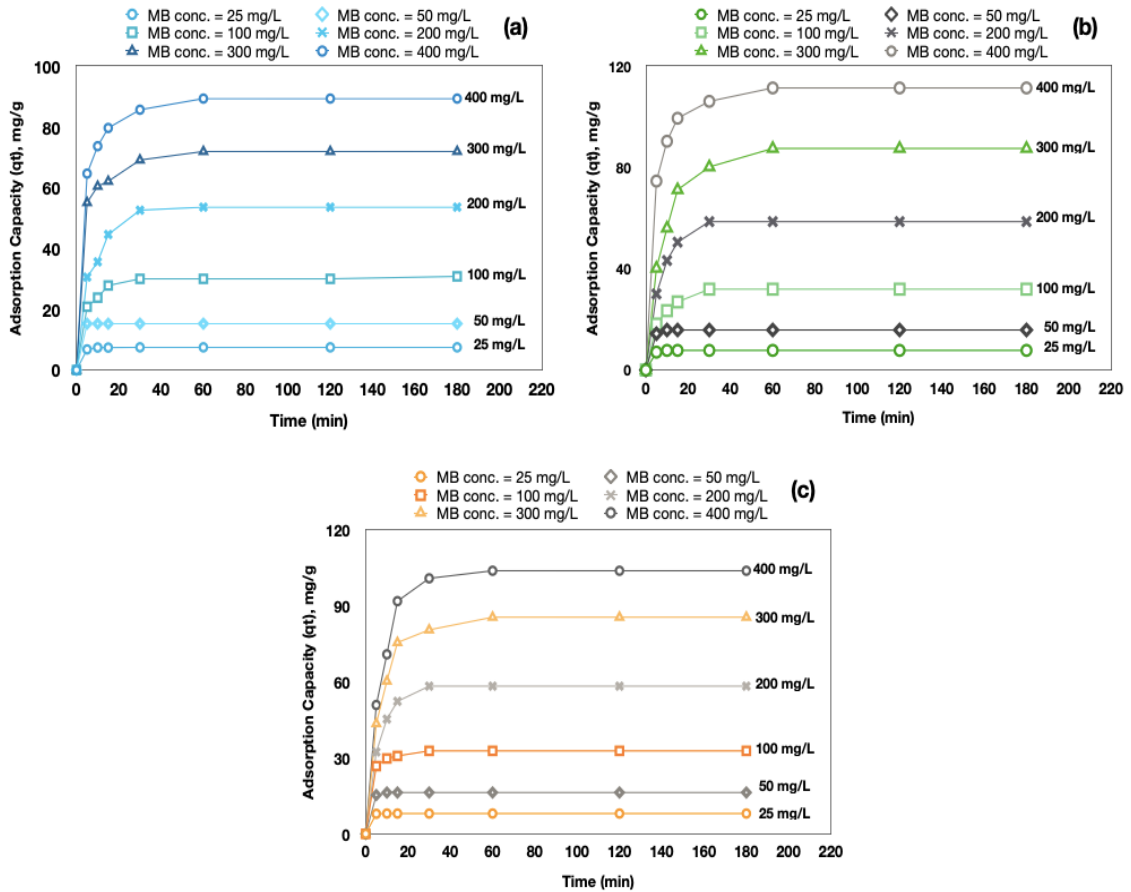


Fig. 5: Effect of contact time on methylene blue adsorption (a) ZnCl_2 -AC, (b) KOH-AC, (c) H_3PO_4 -AC (adsorbent dose = 3 g/L, stirring speed = 120 rpm, temperature = 27 ± 1 °C, volume of solution = 100 mL).

Figure 5a displays that the time to attain equilibrium was observed to be 10 min for 25 and 50 mg/L, whereas this increased to 60 min for a concentration of 300 and 400 mg/L. The increasing trend stopped once a state of equilibrium was achieved. At this stage, the quantity of MB was not significantly changed with time, which indicates that time is sufficient to accomplish equilibrium for the maximum elimination of dye from aqueous solutions by ZnCl_2 -AC. A significant amount of dye was removed by KOH-AC (Fig. 5b) in the first 30 min of contact time due to the existence of a huge number of active sites on the surface of activated carbon. The adsorption equilibrium of methylene blue adsorption on KOH-AC increased from 7.75 to 111.36 mg/g as the initial concentration of methylene blue increased from 25 to 400 mg/L. Methylene blue adsorption onto the H_3PO_4 -AC (Fig. 5c) followed a similar trend as methylene blue adsorption onto ZnCl_2 -AC. At the equilibrium, the adsorption capacity increased from 8.02 to 103.86 mg/g, while the removal percentage dropped from 98.97 to 77.86 % with a rise in the initial methylene blue concentrations from 25 to 400 mg/L (see Fig. 4).

Generally, the equilibrium was achieved within approximately the first hour of adsorption, indicating a favorable interaction between the methylene blue dye and BFS-ACs. These results were similar to those reported by some previous studies [8,15,25,46].

3.3 Adsorption Isotherms Models

Adsorption isotherms have been used to illustrate how the adsorbate molecules distribute between the liquid and solid phases. That is generally significant for the adsorption system design [12]. Adsorption isotherms results are typically presented as a plot of the adsorbed chemical concentration (mg/g) versus the remainder of the solution concentration (mg/L). In this study, the data of adsorption equilibrium was modeled to Langmuir and Freundlich isotherms.

3.3.1 Langmuir Isotherm

The Langmuir isotherm model suggests single-layer surface sorption with no transmigration of the sorbate on the surface without interplaying the sorbed molecules and the uniform energy of absorption [47]. Equation 7 describes the linear form of the Langmuir model and a plot of C_e/q_e against C_e is presented in Fig. 6. The slope and the interception are used to evaluate the maximum adsorption capacity (q_m) and the adsorption rate (K_L), respectively.

$$\frac{C_e}{q_e} = \frac{1}{q_m K_L} + \frac{C_e}{q_m} \quad (7)$$

where K_L (L/mg) and q_m (mg/g) are Langmuir constants related to rate of adsorption and adsorption capacity, respectively. C_e is the equilibrium concentration of the adsorbate (mg/L).

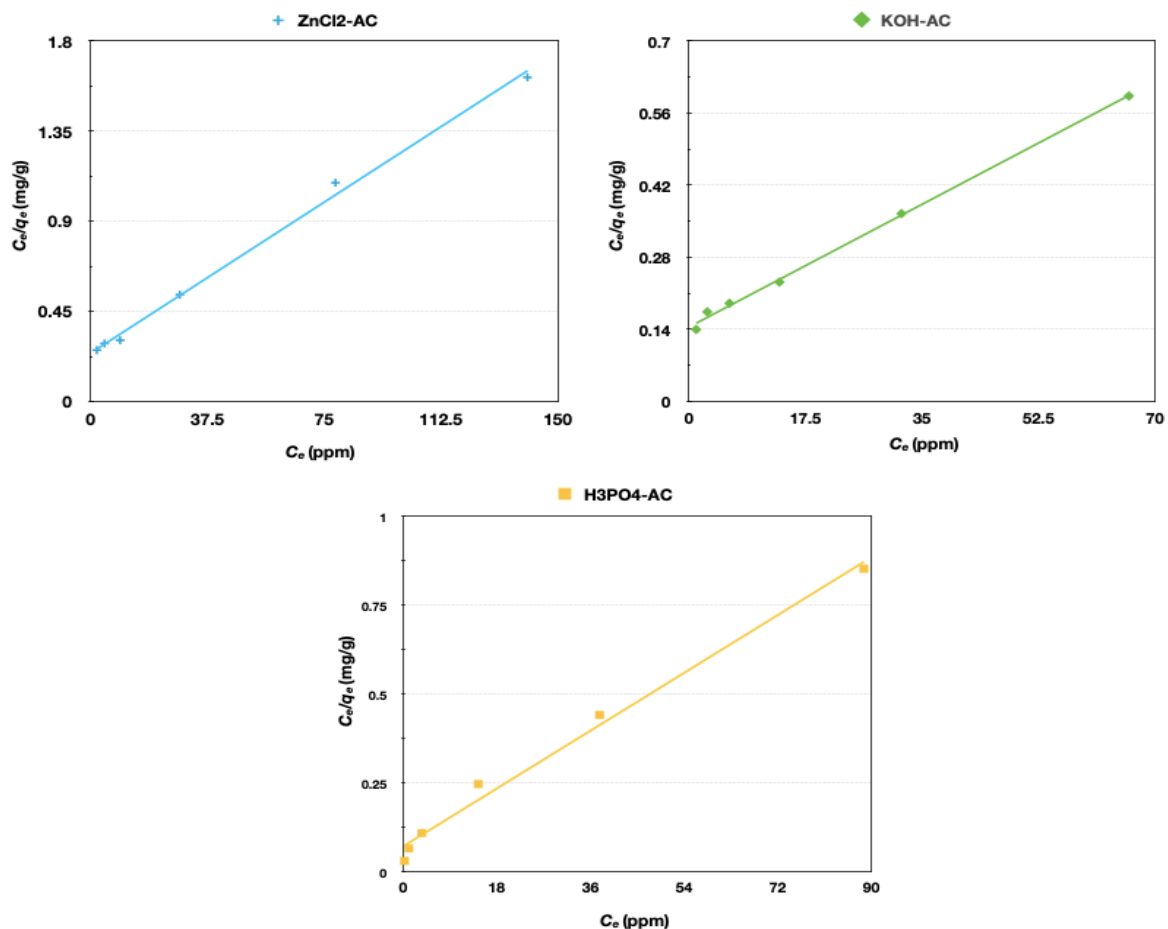


Fig. 6: Langmuir isotherm plot for the removal of methylene blue at 27±1 °C.

3.3.2 Freundlich Isotherm

The Freundlich isotherm is an empirical model based on the heterogeneous surface adsorption and on working sites with various energies [48]. The following equation indicates the linear form of the Freundlich isotherm:

$$\log q_e = \log K_F + \frac{1}{n} \log C_e \quad (8)$$

where q_e is the amount of MB adsorbed at equilibrium (mg/g); C_e is the equilibrium concentration of the adsorbate (mg/L); K_F ((mg/g) (L/mg)^{1/n}) and n are Freundlich constants relating respectively to the adsorption capacity of the adsorbate and the favorability of adsorption process. If the value of $1/n$ is less than 1, the adsorption is favorable.

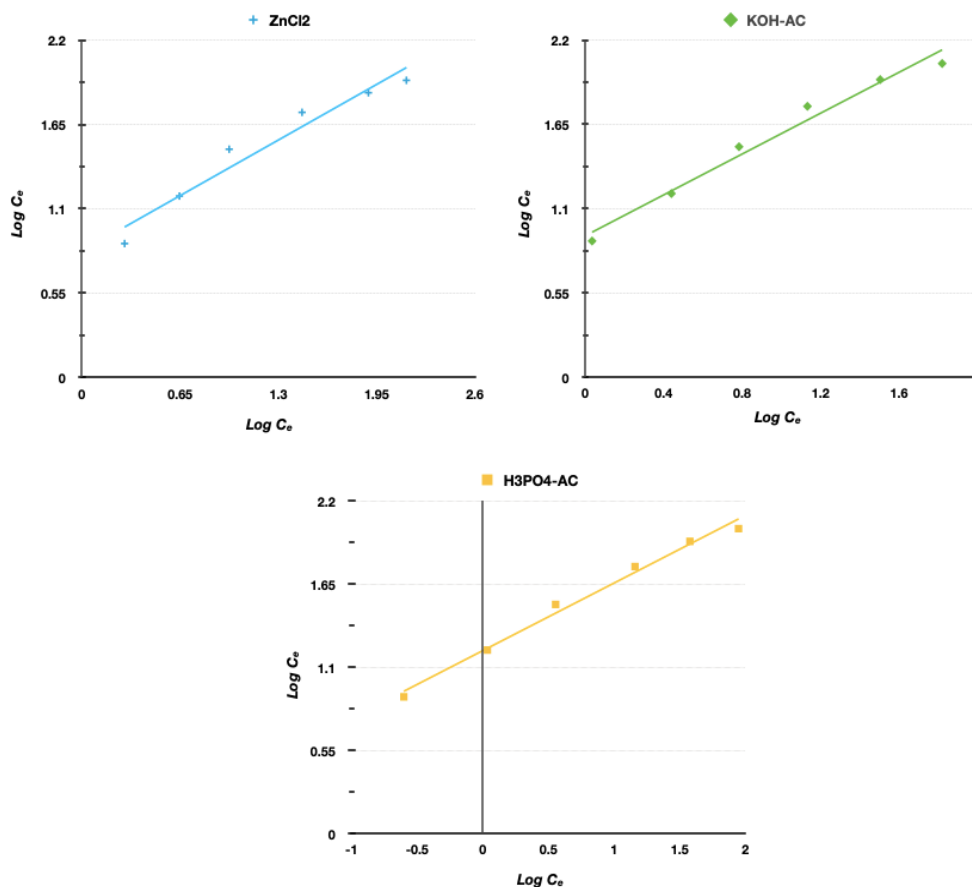


Fig. 7: Freundlich isotherm plot for removal of methylene blue onto synthesized BFS-ACs at 27±1 °C.

Table 2: Isotherm model parameters and correlation coefficients of MB adsorption onto synthesized BFS-ACs at 27±1 °C

| Adsorbent | Langmuir parameters | | | Freundlich parameters | | | |
|------------------------------------|---------------------|-----------------|--------|--------------------------------------|-----------------|-------|--------|
| | K_L (L/mg) | q_m (mg/g) | R^2 | K_F (mg/g)(L/mg) ^{1/n} | $1/n$ (L/mg) | n | R^2 |
| ZnCl ₂ -AC | 0.044 | 90.45 | 0.9963 | 6.663 | 0.557 | 1.793 | 0.9506 |
| H ₃ PO ₄ -AC | 0.1262 | 109.98 | 0.9891 | 13.188 | 0.446 | 2.238 | 0.9888 |
| KOH-AC | 0.060 | 113.63 | 0.9978 | 8.388 | 0.666 | 1.501 | 0.9770 |

Table 2 lists all parameters and determination coefficients (R^2) of MB adsorption on BFS-ACs. For the Freundlich isotherm, the slope $1/n$ of 0 to 1 tests the adsorption intensity or surface heterogeneity of the adsorption and is increasingly heterogeneous as its value reaches nil. A value of $1/n$ lower than 1 suggests a normal Freundlich isotherm, whereas $1/n$ higher than 1 suggests stronger sorption strength [49,50]. The results of adsorption processes showed that the values of $1/n$ were 0.557, 0.446, and 0.666 for $ZnCl_2$, H_3PO_4 , and KOH, respectively, indicating that the conditions of adsorption in this study are favorable. It could be observed that H_3PO_4 showed stronger affinity and greater heterogeneity for MB than $ZnCl_2$ and KOH.

Based on the R^2 , the Langmuir model produced a better fit for the experimental data with higher R^2 for the three produced activated carbons, indicating that the adsorption process occurred on a uniform surface and there was no transmigration of the MB dyes. Therefore, the methylene blue adsorption onto the adsorbent tended to monolayer adsorption. Furthermore, the Langmuir model shows that the maximum adsorption capacities (q_m) were 90.45 mg/g, 109.98 mg/g, and 113.63 mg/g for $ZnCl_2$, H_3PO_4 , and KOH, respectively. These agree well with the experimental results, which also showed that the adsorption process was in line with the Langmuir model. Table 3 shows a comparison of the maximum sorption capacities of the methylene blue with other reported values for some agricultural by-products based activated carbons. The findings from this table showed that BFS-ACs can effectively be used for the removal of MB dyes from the aqueous resolution with a great absorption capacity compared to many other sorbents.

Table 3: A comparison of maximum adsorption of methylene blue onto activated carbons produced from different precursors

| Precursor | Activating agent | Adsorption capacity (mg/g) | References |
|--|------------------|----------------------------|------------|
| Cashew nutshell | KOH | 68.72 | [51] |
| Pineapple waste biomass | $ZnCl_2$ | 288.34 | [52] |
| Coconut (<i>Cocos nucifera</i>) Leaf | H_3PO_4 | 250 | [53] |
| Wood | KOH | 59.92 | [54] |
| Corn cob residue | H_3PO_4 | 183.3 | [55] |
| Baobab fruit shell | H_3PO_4 | 334.45 | [18] |
| Baobab fruit shell | $ZnCl_2$ | 90.45 | This Study |
| | H_3PO_4 | 109.98 | |
| | KOH | 113.63 | |

3.4 Adsorption Kinetic Studies

The time-dependent experimental data were evaluated in order to investigate the rate-limiting step by adapting them to different kinetic models, namely the pseudo-first order model [56] and the pseudo-second order model [57]. Linear forms of pseudo-first order and pseudo-second-order kinetic equations are represented by Equations (9) and (10), respectively.

$$\ln(q_e - q_t) = \ln q_e - k_1 t \quad (9)$$

$$\frac{t}{q_t} = \frac{1}{(k_2 q_e^2)} + \frac{1}{q_e} t \quad (10)$$

where k_1 (min^{-1}) and k_2 ($\text{g}/\text{min}/\text{mg}$) are the rate constant of the pseudo-first order and pseudo second-order adsorption, q_e (mg/g) and q_t (mg/g) are the amounts of MB adsorbed onto BFS-ACs at the equilibrium and at any time t (min).

The values of first-order rate constants (k_1) and the equilibrium adsorption capacities (q_e) were determined from the slope and intercept of the plots of $\ln(q_e - q_t)$ against t , respectively. While the second-order sorption rate constants (k_2) and the equilibrium adsorption capacities (q_e) were determined from the slopes and intercepts of the plots of t/q_t versus t . Table 4 lists the derived kinetic parameters for the pseudo-first and pseudo-second order. From Table 4, the values of the rate constant pseudo-first-order model did not follow any particular pattern and the equilibrium adsorption capacities ($q_e \text{ cal}$) were quite different and not in agreement with experimental data, and the correlation coefficients (R^2) of the pseudo-first order model were low values. On the other hand, the correlation coefficients (R^2) of the pseudo-second-order model are close or equal to 1 for all initial concentrations of the different carbons prepared, indicating that the experimental kinetic data fitted the pseudo-second-order model better (see Table 4). Furthermore, the equilibrium adsorption capacities calculated ($q_e \text{ cal}$) values that were obtained from the second-order equations are very similar to equilibrium adsorption capacities experimental ($q_e \text{ exp}$), suggesting that the second-order model is more suitable for the kinetics of the methylene blue and the rate-limiting step of MB onto BFS-ACs may be chemisorption. The rate constant (k_2) values decrease with the initial methylene blue concentration increasing owing to the lower competition for the sorption surface sites at lower concentrations [51].

Table 4: Kinetic model parameters and correlation coefficients for adsorption of MB onto ZnCl_2 -AC, H_3PO_4 -AC, and KOH-AC

| Adsorbent | C_0 (ppm) | $q_e \text{ exp}$ (mg/g) | Pseudo-first-order kinetics | | | Pseudo-second-order kinetics | | |
|--------------------------------|----------------|-----------------------------|-----------------------------|--------------|--------|------------------------------|---------------------|--------|
| | | | $q_e \text{ cal}$ (mg/g) | k_1 (/min) | R^2 | $q_e \text{ cal}$ (mg/g) | k_2 (g/min/mg) | R^2 |
| ZnCl ₂ | 25 | 7.472 | 0.00680 | 0.0297 | 0.51 | 7.4794 | 0.8392 | 1 |
| | 50 | 15.252 | 0.00023 | 0.0204 | 0.22 | 15.2671 | 1.3000 | 1 |
| | 100 | 30.805 | 35.1803 | 0.0306 | 0.74 | 30.8641 | 0.0187 | 0.9996 |
| | 200 | 53.583 | 36.8468 | 0.051 | 0.69 | 54.6448 | 0.0072 | 0.9993 |
| | 300 | 71.916 | 52.7351 | 0.0442 | 0.74 | 72.4637 | 0.0100 | 0.9998 |
| | 400 | 89.302 | 59.2788 | 0.0555 | 0.69 | 90.0900 | 0.0079 | 0.9999 |
| KOH | 25 | 7.750 | 0.000040 | 0.1015 | 0.2254 | 7.7579 | 1.3962 | 1 |
| | 50 | 15.805 | 0.0039 | 0.0217 | 0.33 | 15.8227 | 0.5547 | 1 |
| | 100 | 31.916 | 2.4027 | 0.0398 | 0.5143 | 32.3624 | 0.0148 | 0.9995 |
| | 200 | 58.583 | 0.2343 | 0.0886 | 0.5335 | 59.5238 | 0.0076 | 0.9993 |
| | 300 | 87.472 | 142.6921 | 0.1052 | 0.719 | 89.2857 | 0.0031 | 0.999 |
| | 400 | 111.361 | 85.9824 | 0.0926 | 0.719 | 112.3595 | 0.0056 | 0.9998 |
| H ₃ PO ₄ | 25 | 8.021 | 0.000037 | 0.0197 | 0.2182 | 8.0192 | 9.7188 | 1 |
| | 50 | 16.311 | 0.000110 | 0.0233 | 0.2252 | 16.3132 | 0.8946 | 1 |
| | 100 | 32.751 | 0.3016 | 0.0473 | 0.5372 | 32.8947 | 0.0486 | 1 |
| | 200 | 58.31 | 5.0944 | 0.0392 | 0.5014 | 59.1715 | 0.0095 | 0.9995 |
| | 300 | 85.521 | 106.1451 | 0.0626 | 0.696 | 86.9565 | 0.0044 | 0.9994 |
| | 400 | 103.861 | 120.0051 | 0.0620 | 0.6974 | 105.2631 | 0.0036 | 0.9992 |

4. CONCLUSION

The present study has put forward that baobab fruit shell is a promising precursor in generating high quality activated carbon at an affordable price. The results showed that KOH was found more effective than the other activating agents ($ZnCl_2$ and H_3PO_4) under the same conditions for the methylene blue removal. According to the results, properties of the activated carbon are significantly influenced by interaction with various chemical agents. Adsorption capacity of the adsorbent was affected by initial Methylene Blue concentration and contact time. SEM micrographs indicate that pores of varying sizes and shapes have been obtained from various active agents. Besides, chemical reagents had a significant effect on the nature of the surface functional groups as shown in FTIR results. The adsorption studies show that the pseudo second order model provided the best description of the kinetic uptake properties. On the other hand, the adsorption isotherms were well described by the Langmuir model. The results indicate that BFS-ACs is an effective adsorbent for MB adsorption from aqueous solutions.

ACKNOWLEDGEMENT

The authors are grateful to the Department of Biotechnology Engineering, Faculty of Engineering, International Islamic University Malaysia (IIUM) for providing continuous support to the research at hand. We are as well thankful to the International Institute for Halal Research and Training (INHART), IIUM for giving us access to FTIR instrument for characterization.

REFERENCES

- [1] Özhan A, Şahin Ö, Küçük MM, Saka C. (2014) Preparation and characterization of activated carbon from pine cone by microwave-induced $ZnCl_2$ activation and its effects on the adsorption of methylene blue. *Cellulose*, 21: 2457-2467. <https://doi.org/10.1007/s10570-014-0299-y>
- [2] Yang J, Qiu K. (2010) Preparation of activated carbons from walnut shells via vacuum chemical activation and their application for methylene blue removal. *Chem Eng J*, 165: 209-217. <https://doi.org/10.1016/j.cej.2010.09.019>
- [3] Koo WK, Gani NA, Shamsuddin MS, Subki NS, Sulaiman MA. (2015) Comparison of wastewater treatment using activated carbon from bamboo and oil palm: an overview. *J Trop Resour Sustain Sci*, 3: 54-60
- [4] Wang LG, Yan GB. (2011) Adsorptive removal of direct yellow 161 dye from aqueous solution using bamboo charcoals activated with different chemicals. *Desalination*, 274: 81-90. <https://doi.org/10.1016/j.desal.2011.01.082>
- [5] Gupta T. (2017) *Carbon: The black, the gray and the transparent*. Springer.
- [6] Gupta VK, Tyagi I, Agarwal S, Singh R, Chaudhary M, Harit A, Kushwaha S (2016) Column operation studies for the removal of dyes and phenols using a low cost adsorbent. *Glob J Environ Sci Manag*, 2: 1-10. <https://doi.org/10.7508/gjesm.2016.01.001>
- [7] Spagnoli AA, Giannakoudakis DA, Bashkova S. (2017) Adsorption of methylene blue on cashew nut shell based carbons activated with zinc chloride: The role of surface and structural parameters. *J Mol Liq*, 229: 465-471. <https://doi.org/10.1016/j.molliq.2016.12.106>
- [8] Sogbochi E. (2017) Evaluation of Adsorption Capacity of Methylene Blue in Aqueous Medium by Two Adsorbents: The raw hull of *lophira lanceolata* and its activated carbon. *Am J Phys Chem*, 6(5): 76-87. <https://doi.org/10.11648/j.ajpc.20170605.11>
- [9] Hameed BH, Din ATM, Ahmad AL. (2007) Adsorption of methylene blue onto bamboo-based activated carbon: Kinetics and equilibrium studies. *J Hazard Mater*, 141: 819-825. <https://doi.org/10.1016/j.jhazmat.2006.07.049>

- [10] Islam MA, Sabar S, Benhouria A, Khanday WA, Asif M, Hameed BH. (2017) Nanoporous activated carbon prepared from karanj (*Pongamia pinnata*) fruit hulls for methylene blue adsorption. *J Taiwan Inst Chem Eng*, 74: 96-104. <https://doi.org/10.1016/j.jtice.2017.01.016>
- [11] Guo J, Song Y, Ji X, Ji L, Cai L, Wang Y, Zhang H, Song W. (2019) Preparation and characterization of nanoporous activated carbon derived from prawn shell and its application for removal of heavy metal ions. *Materials*, 12(2): 1-17. <https://doi.org/10.3390/ma12020241>
- [12] Gao J, Kong D, Wang Y, Wu J, Sun S, Xu P. (2013a) Production of mesoporous activated carbon from tea fruit peel residues and its evaluation of methylene blue removal from aqueous solutions. *BioResources*, 8: 2145-2160. <https://doi.org/10.15376/biores.8.2.2145-2160>
- [13] Gao JJ, Qin YB, Zhou T, Cao DD, Xu P, Hochstetter D, Wang YF. (2013b) Adsorption of methylene blue onto activated carbon produced from tea (*Camellia sinensis* L.) seed shells: Kinetics, equilibrium, and thermodynamics studies. *J Zhejiang Univ Sci B*, 14: 650-658. <https://doi.org/10.1631/jzus.B12a0225>
- [14] Vicinisvarri I, Shanker Kumar S, Nor Aimi AW, Norain I, Nurul Izza H. (2014) Preparation and characterization of phosphoric acid activated carbon from *Canarium odontophyllum* (Dabai) nutshell for methylene blue adsorption. *Res J Chem Environ*, 18: 57-62
- [15] Banat F, Al-Asheh S, Makhadmeh L. (2003) Preparation and examination of activated carbons from date pits impregnated with potassium hydroxide for the removal of methylene blue from aqueous solutions. *Adsorpt Sci Technol*, 21: 597-606. <https://doi.org/10.1260/026361703771953613>
- [16] Ndi Nsami J, Ketcha Mbadcam J. (2013) The adsorption efficiency of chemically prepared activated carbon from cola nut shells by $ZnCl_2$ on methylene blue. *J Chem*, 2013: 1-7. <https://doi.org/10.1155/2013/469170>
- [17] Idris-Hermann KT, Raoul TTD, Giscard D, Gabche AS. (2018) Preparation and characterization of activated carbons from bitter kola (*Garcinia kola*) nut shells by chemical activation method using H_3PO_4 , KOH and $ZnCl_2$. *Chem Sci Int J*, 23: 1-15. <https://doi.org/10.9734/csji/2018/43411>
- [18] Vunain E, Biswick T. (2018) Adsorptive removal of methylene blue from aqueous solution on activated carbon prepared from Malawian baobab fruit shell wastes: Equilibrium, kinetics and thermodynamic studies and thermodynamic studies. *Sep Sci Technol*, 54(1): 1-15. <https://doi.org/10.1080/01496395.2018.1504794>
- [19] García JR, Sedran U, Zaini MAA, Zakaria ZA. (2018) Preparation, characterization, and dye removal study of activated carbon prepared from palm kernel shell. *Environ Sci Pollut Res*, 25: 5076-5085. <https://doi.org/10.1007/s11356-017-8975-8>
- [20] Sahira J, Mandira A, Prasad PB, Ram PR. (2013) Effects of activating agents on the activated carbons prepared from Lapsi seed stone. *Res J Chem Sci*, 3: 19-24
- [21] Bedin KC, Martins AC, Cazetta AL, Pezoti O, Almeida VC. (2016) KOH-activated carbon prepared from sucrose spherical carbon: Adsorption equilibrium, kinetic and thermodynamic studies for Methylene Blue removal. *Chem Eng J*, 286: 476-484. <https://doi.org/10.1016/j.cej.2015.10.099>
- [22] Hong Tan Y, Xian Chin S, Lun Ang W, Mahmoudi E, Mohd Zainoodin A, Mohammad AW. (2018) Effect of H_3PO_4 and KOH as the Activating agents on the synthesis of low-cost activated carbon from duckweeds plants. *J Kejuruter*, 1(4): 37-43. [https://doi.org/10.17576/jkukm-2018-si1\(4\)-05](https://doi.org/10.17576/jkukm-2018-si1(4)-05)
- [23] Baccar R. (2013) Removal of some water contaminants by adsorption on activated carbon prepared from olive-waste cakes and biological treatment using fungi. PhD thesis. Sfax University, Chemical Engineering Department.
- [24] Hayashi J, Horikawa T, Muroyama K, Gomes VG. (2002) Activated carbon from chickpea husk by chemical activation with K_2CO_3 : Preparation and characterization. *Microporous Mesoporous Mater*, 55: 63-68. [https://doi.org/10.1016/S1387-1811\(02\)00406-7](https://doi.org/10.1016/S1387-1811(02)00406-7)
- [25] Ben Nasr J, Hamdi N, Elhalouani F. (2017) Characterization of activated carbon prepared from sludge paper for methylene blue adsorption. *J Mater Environ Sci*, 8: 1960-1967
- [26] Alcañiz-Monge J, Illán-Gómez MJ. (2008) Insight into hydroxides-activated coals: Chemical or physical activation? *J Colloid Interface Sci*, 318: 35-41. <https://doi.org/10.1016/j.jcis.2007.10.017>

- [27] Martins AC, Pezoti O, Cazetta AL, Bedin KC, Yamazaki DAS, Bandoch GFG, Asefa T, Visentainer JV, Almeida VC. (2015) Removal of tetracycline by NaOH-activated carbon produced from macadamia nut shells: Kinetic and equilibrium studies. *Chem Eng J*, 260: 291-299. <https://doi.org/10.1016/j.cej.2014.09.017>
- [28] Dzigbor A, Chimphango A. (2019) Production and optimization of NaCl-activated carbon from mango seed using response surface methodology. *Biomass Convers Biorefinery*, 9: 421-431. <https://doi.org/10.1007/s13399-018-0361-3>
- [29] Kabbashi NA, Mirghani MES, Alam MZ, Qudsieh SY, Bello IA. (2017) Characterization of the Baobab fruit shells as adsorption material. *Int Food Res J*, 24: 472-474.
- [30] Ofomaja AE. (2007) Sorption dynamics and isotherm studies of methylene blue uptake on to palm kernel fibre. *Chem Eng J*, 126: 35-43. <https://doi.org/10.1016/j.cej.2006.08.022>
- [31] Al-Khatib MFR, Munjid M. (2011) Production of activated carbon from palm oil empty fruit bunch by chemical activation. in: *Current research and developments in biotechnology engineering at IIUM*. IIUM Press, Kuala Lumpur, pp 209-216
- [32] Milne T, Brennan AH, Glenn BH. (1990) *Sourcebook of methods of analysis for biomass and biomass conversion processes*. Springer Science & Business Media.
- [33] American Society for Testing and Materials. (1991) *Standard for method for moisture in activated carbon ASTM D 2867-91*. PA: ASTM Committee on Standards, Philadelphia
- [34] Prahas D, Kartika Y, Indraswati N, Ismadji S. (2008) Activated carbon from jackfruit peel waste by H₃PO₄ chemical activation: Pore structure and surface chemistry characterization. *Chem Eng J*, 140: 32-42. <https://doi.org/10.1016/j.cej.2007.08.032>
- [35] J Hassen JH. (2017) Effect of KOH ratio on the formation of activated carbon from pressed wood residues. *Int J Pharm Sci Res*, 8: 4875-4880. [https://doi.org/10.13040/IJPSR.0975-8232.8\(11\)4875-80](https://doi.org/10.13040/IJPSR.0975-8232.8(11)4875-80)
- [36] Vunain E, Kenneth D, Timothy B. (2017) Synthesis and characterization of low-cost activated carbon prepared from Malawian baobab fruit shells by H₃PO₄ activation for removal of Cu (II) ions: equilibrium and kinetics studies. *Appl Water Sci*, 7: 4301-4319. <https://doi.org/10.1007/s13201-017-0573-x>
- [37] Nunes CA. (2011) Estimation of surface area and pore volume of activated carbons by methylene blue and iodine numbers. *Quim Nova*, 34(3): 472-476. <https://doi.org/10.1590/S0100-40422011000300020>
- [38] Mona S, Kaushik A, Kaushik CP. (2011) Biosorption of reactive dye by waste biomass of *Nostoc linckia*. *Ecol Eng*, 37: 1589-1594. <https://doi.org/10.1016/j.ecoleng.2011.04.005>
- [39] Gottipati R. (2012) *Preparation and characterization of microporous activated carbon from biomass and its application in the removal of chromium (VI) from aqueous phase*. PhD thesis. Natl Inst Technol Rourkela Odisha, India. Department of Chemical Engineering.
- [40] Abdullah AH, Kassim A, Zainal Z, Mohd Zobir H, Kuang D, Wooi SO, Ahmad F. (2001) Preparation and characterization of activated carbon from Gelam wood bark (*Melaleuca cajuputi*) *Malaysian J Anal Sci*, 7: 65-68
- [41] Marsh H, Rodríguez F. (2006) *Activated Carbon*. Elsevier
- [42] Jawad AH, Abdulhameed AS. (2020) Statistical modeling of methylene blue dye adsorption by high surface area mesoporous activated carbon from bamboo chip using KOH-assisted thermal activation. *Energy, Ecol Environ*, 5: 456-469. <https://doi.org/10.1007/s40974-020-00177-z>
- [43] Puziy AM, Poddubnaya OI, Martínez-Alonso A, Suárez-García F, Tascón JMD. (2005) Surface chemistry of phosphorus-containing carbons of lignocellulosic origin. *Carbon N Y*, 43: 2857-2868. <https://doi.org/10.1016/j.carbon.2005.06.014>
- [44] Kumar A, Jena HM. (2016) Removal of methylene blue and phenol onto prepared activated carbon from Fox nutshell by chemical activation in batch and fixed-bed column. *J Clean Prod*, 137: 1246-1259. <https://doi.org/10.1016/j.jclepro.2016.07.177>
- [45] De La Luz-Asunción M, Sánchez-Mendieta V, Martínez-Hernández AL, Castaño VM, Velasco-Santos C. (2015) Adsorption of phenol from aqueous solutions by carbon nanomaterials of one and two dimensions: Kinetic and equilibrium studies. *Journal of Nanomaterials*. <https://doi.org/10.1155/2015/405036>

- [46] Dural MU, Cavas L, Papageorgiou SK, Katsaros FK. (2011) Methylene blue adsorption on activated carbon prepared from *Posidonia oceanica* (L.) dead leaves: Kinetics and equilibrium studies. *Chem Eng J*, 168: 77-85. <https://doi.org/10.1016/j.cej.2010.12.038>
- [47] Vimala R, Das N. (2009) Biosorption of cadmium (II) and lead (II) from aqueous solutions using mushrooms: A comparative study. *J Hazard Mater*, 168: 376-382. <https://doi.org/10.1016/j.jhazmat.2009.02.062>
- [48] Kilic M, Apaydin-Varol E, Pütün AE. (2011) Adsorptive removal of phenol from aqueous solutions on activated carbon prepared from tobacco residues: Equilibrium, kinetics and thermodynamics. *J Hazard Mater*, 189: 397-403. <https://doi.org/10.1016/j.jhazmat.2011.02.051>
- [49] Angin D, Altintig E, Köse TE. (2013) Influence of process parameters on the surface and chemical properties of activated carbon obtained from biochar by chemical activation. *Bioresour Technol*, 148: 542-549. <https://doi.org/10.1016/j.biortech.2013.08.164>
- [50] Angin D. (2014) Utilization of activated carbon produced from fruit juice industry solid waste for the adsorption of Yellow 18 from aqueous solutions. *Bioresour Technol*, 168: 259-266. <https://doi.org/10.1016/j.biortech.2014.02.100>
- [51] Kumar PS, Ramalingam S, Sathishkumar K. (2011) Removal of methylene blue dye from aqueous solution by activated carbon prepared from cashew nut shell as a new low-cost adsorbent. *Korean J Chem Eng*, 28: 149-155. <https://doi.org/10.1007/s11814-010-0342-0>
- [52] Mahamad MN, Zaini MAA, Zakaria ZA. (2015) Preparation and characterization of activated carbon from pineapple waste biomass for dye removal. *Int Biodeterior Biodegrad*, 102: 274-280. <https://doi.org/10.1016/j.ibiod.2015.03.009>
- [53] Jawad AH, Sabar S, Ishak MAM, Wilson LD, Ahmad Norrahma SS, Talari MK, Farhan AM. (2017) Microwave-assisted preparation of mesoporous-activated carbon from coconut (*Cocos nucifera*) leaf by H_3PO_4 activation for methylene blue adsorption. *Chem Eng Commun*, 204: 1143-1156. <https://doi.org/10.1080/00986445.2017.1347565>
- [54] Danish M, Ahmad T, Hashim R, Said N, Akhtar MN, Mohamad-Saleh J, Sulaiman O. (2018) Comparison of surface properties of wood biomass activated carbons and their application against rhodamine B and methylene blue dye. *Surfaces and Interfaces*, 11: 1-13. <https://doi.org/10.1016/j.surfin.2018.02.001>
- [55] Jawad AH, Bardhan M, Islam MA, M.A. Islam, Syed-Hassan SSA, Surip SN, Alothman ZA, Khan MR. (2020) Insights into the modeling, characterization and adsorption performance of mesoporous activated carbon from corn cob residue via microwave-assisted H_3PO_4 activation. *Surfaces and Interfaces*, 21:100688. <https://doi.org/10.1016/j.surfin.2020.100688>
- [56] Budinova T, Ekinici E, Yardim F, Grimm A, Björnbohm E, Minkova V, Goranova M. (2006) Characterization and application of activated carbon produced by H_3PO_4 and water vapor activation. *Fuel Process Technol*, 87: 899-905. <https://doi.org/10.1016/j.fuproc.2006.06.005>
- [57] Ho YS, McKay G. (1999) Pseudo-second order model for sorption processes. *Process Biochem*, 34: 451-465. <https://doi.org/10.1021/acs.oprd.7b00090>